VISCOSITY OF SHOCK-COMPRESSED FLUIDS

L. V. Al'tshuler, G. S. Doronin,
and G. Kh. Kim

UDC 532.11:539.8

Estimations of the viscosity η behind shockwaves in the majority of cases are made by the impurity conductivity λ of weak electrolytes. On the basis of the Walden [6] rule about the constancy of the product $\eta\lambda$, it follows that for water [1, 2] and a large group of organic compounds [3-5] the viscosity of methanol, formamide, ethanol, butanol, nitromethane, and water remains at the same level for 6-9 GPa as under normal conditions, grows several time for n-methyl formamide, acetone, and glycerine, and increases by approximately an order for dimethyl formamide (DMF), dimethyl sulfoxide, nitrobenzene, and nitroglycerine.

The viscosity for shock-compressed water has been determined by several methods: by the corrugated front method [7, 8], i.e., by the spoilage of the similarity in the damping of perturbations with different wavelength: by recording the acceleration modes of heavy cylinders behind the shockfront in [9, 10], by the width of the wave front [11], and by the rate of sulfur particle coagulation [12]. The different methods resulted in a dramatic difference in the results. While the viscosity of water at 8-22 GPa pressures remained at the level of centipoise units according to conductivity data, it grew six orders at the same pressures according to the corrugated front method, i.e., to 10^4 P. In investigations [9] of cylinder entrainment by a free-stream of shock-compressed water at 3-8 GPa, the description of the experiments reached 10^3 P for the viscosity and in the modified method [10] by using especially thin cylindrical sensors $\eta \sim$ 10-20 P. According to [5, 10], there was a systematic error in [9], caused by a large transition period to build up the quasistationary flow mode whose duration is proportional to the cylinder diameter and comparable with the total recording time in [9]. Consequently, the data of [10], which still exceed the estimates of [1] based on impurity conductivity measurements by three orders of magnitude are more confident. The contradiction detected indicates the spoilage of the Walden rule for shock-compressed water because of the difference in the mechanisms and factors governing the ion mobility and the structural viscosity of water.

An experimental foundation for the method of determining the viscosity of shock-compressed fluids by the acceleration of heavy cylinders behind a shock front and new results of measuring the viscosity coefficient in DMF, glycerine, and water are presented in this paper and confirm the non-conservation of the Walden rule for water.

Method of Investigation

The experimental realization of the method of accelerating cylinders (AC) in [9, 10] is based on continuous electromagnetic recording [13] of regimes of cylindrical conductor velocity growth as a fluid moving behind a shock front flows around them. The correctness of the AC method is established by a direct comparison of the static and dynamic values of the viscosity under identical pressures and temperatures.

A shock with the amplitude ~1 GPa needed for this purpose, a rectangular profile, and high wave front symmetry was produced in the liquid by the impact of a polyfluorethylene resin piston of 80 mm diameter accelerated by a high-velocity gun. The fluxes of compressed substance obtained by such a method had velocities of several hundreds of meters per second, determined by flat aluminum foil sensors 0.06 mm thick and 10 × 10 mm in size. The flux velocity sensors and the cylindrical conductors were placed side by side in a homogeneous magnetic field of 450 Oe intensity.

The possibilities of the method that reflects the relation between the rheological characteristics of the medium and the acceleration mode of the cylinders are illustrated in Figs. 1 and 2, where results are given of tests with water and glycerine for a different initial temperature. Each test in Fig. 1 is represented by two oscillograms with fluid velocity

Moscow. Translated from Zhurnal Prikladnoi Mekhaniki i Tekhnicheskoi Fiziki, No. 6, pp. 110-118, November-December, 1986. Original article submitted March 28, 1985.

0021-8944/86/2706-0887$12.50

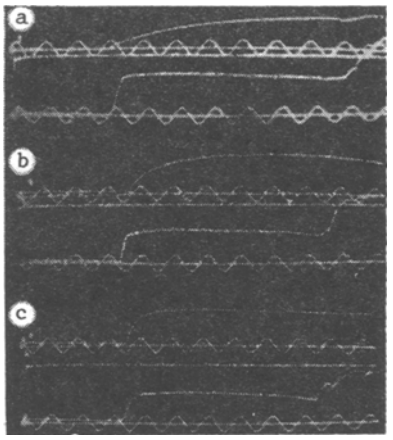

Fig. 1

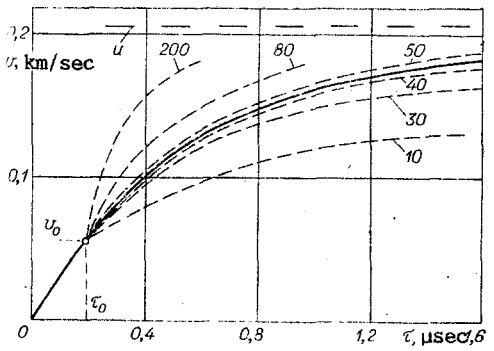

Fig. 2

recordings and the velocity growth of a tungsten cylindrical conductor of 0.030 mm diameter. The timing marker frequency is 1 MHz. The upper reading in Fig. 1a determines the comparatively slow entrainment of the cylinder by compressed water with an initial temperature t_0 = 6°C and viscosity $\eta_0 = 1.48 \cdot 10^{-2}$ P [14]. The velocity of water motion is u = 0.430 km/sec for p = 1.0 GPa. An analogous oscillogram in Fig. 1b with a more rapid set of cylinder velocities refers to glycerine with t_0 = 48°C, η_0 = 1.98 P, p = 1.24 GPa, u = 0.46 km/sec and in Fig. 1c to glycerine pre-cooled to $t_0 = -10$°C with η_0 = 340 P, p = 1.12 GPa, u = 0.33 km/sec (the value of η_0 for glycerine is presented in [15]). Because of the high viscosity, the configurations of the plane and cylindrical sensor acceleration curves in Fig. 1c are indistinguishable since the velocity growth occurs in both cases in the wave front in a time proportional to the width of the viscous discontinuity [16]. For glycerine at the temperature 18°C (η_0 = 18 P), the graph of cylinder velocity growth behind the shock front (p = 0.63 GPa, ρ = 1.383 g/cm^3, and u = 0.21 km/sec) is displayed by the solid line in Fig. 2.

Determination of the viscosity by the AC method is realized by comparing the experimental curves with the computed τ trajectories that are functionally dependent on the viscosity. According to [10, 17], the cylinder acceleration is described by the expression

$$\frac{dv}{d\tau} = \frac{\rho}{\pi r(\rho_1 + \rho)}(u - v)^2 \Psi(\mathrm{Re}) + 4\frac{\sqrt{\pi\eta\rho}}{\rho_1 + \rho} r\left[\frac{u}{\sqrt{\tau}} - \int_0^{\tau} \frac{dv}{d\tau_1}\frac{d\tau_1}{\sqrt{\tau - \tau_1}}\right], \qquad (1)$$

where ρ_1, r, v are the density, radius, and variable velocity of the cylinder in the compressed fluid; ρ, u are the fluid flow density and velocity; τ is the time measured from the beginning of cylinder motion; τ_1 $(0 < \tau_1 \leq \tau)$ is the integration variable; η is the dynamic viscosity coefficient; $\mathrm{Re} = 2\rho r(u - v)/\eta$ is the Reynolds number; $\Psi(\mathrm{Re})$ is the resistance function according to [18]. As analysis showed [10], the first term in the right side of (1) is dominant and describes the cylinder acceleration in the stationary flow mode with the apparent mass taken into account. The second term in (1) refers to the Hereditary Basse force that reflects the process of boundary layer formation for nonstationary flows. The initial conditions for v_0, τ_0 for the integration of (1) are determined by the coordinates of the experimental acceleration curve at an arbitrarily selected point of the trajectory arranged after completion of the transition period τ_0. The duration τ_0 is ~0.1 μsec for thin cylinders. The configuration of the experimental dependence $\Psi(\mathrm{Re})$ [18], approximated by the polynomial $\log\Psi(\mathrm{Re}) = 1.03 - 0.683x + 0.073x^2 + 0.038x^3 - 0.008x^4$, where $x = \log \mathrm{Re}$, allows determination of the viscosity by the AC method in the $0.1 \leq \mathrm{Re} \leq 250$ interval.

For the specific conditions of the test in Fig. 2, the experimental acceleration curve is compared with the shaded network of computed $v(\tau)$ dependences calculated for different viscosity coefficients (the numbers at the curves). The computation for η = 50 P passes somewhat above the experiment and for η = 40 P somewhat below. The actual viscosity of glycerine is constrained by these limits. The results of this test and of other experiments performed for t_0 = 19 ± 2°C and p = 2.4 GPa are shown by vertical segments in a semi-logarithmic scale in the coordinates $\log\eta - p$ in Fig. 3, where the domain of probable values of the viscosity from the experiments is bounded by the dashed lines.

The adequacy of the viscosity determinations obtained by the AC method is set up by comparing them with the static measurements executed in [4] in nearby pressure and temperature

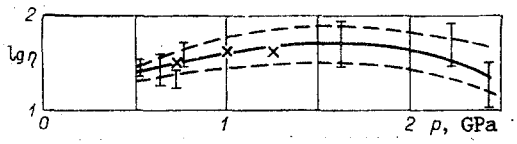

Fig. 3

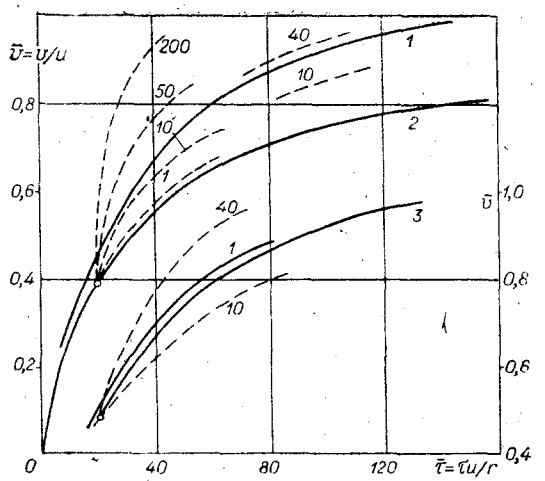

Fig. 4

ranges. Independent information about the viscosity and the impurity electrical conductivity at 20, 80, and 150°C temperatures under static compression, and the impurity conductivity in dynamic tests is obtained to a 1.5 GPa pressure in this paper. Comparing the "static" and "dynamic" impurity conductivities afforded a possibility of finding the shock heating temperature with high accuracy, and then the viscosity of the shock-compressed glycerine from static measurements by means of the Hugoniot p–T states obtained. Description and extrapolation of the data [4] in the Hugoniot temperature were performed by means of the relationship

$$T = T_0 + 106u + 87u^2, \qquad (2)$$

where u is the fluid velocity behind the shock front, km/sec, and T_0 is the initial temperature, °K.

For the p–T-states of the adiabat obtained in such a manner the viscosities from static data and their nearby extrapolation to 2.4 GPa are represented in Fig. 3 by solid lines (the crosses are the results of estimating η by means of the conductivity).

As Figs. 1 and 3 show, experimental recordings of the acceleration modes of thin cylinders realistically reflect the rheological characteristics of compressed fluids, and their interpretation by the method elucidated leads to results that agree with the traditional methods of determining the viscosity and with data on the conductivity of glycerine. A similar agreement between the estimates obtained by the AC and impurity conductivity methods holds for glycerine even at high pressures (6-8 GPa).

The materials presented show that at compressed fluid flow velocities from 0.2-2.0 km/sec the AC method allows the determination of the viscosity with 30-50% possible deviations in a range from several to 100-200 P. Application of the method for high shock amplitudes is constrained by the appearance of the intrinsic conductivity of the fluid. For water, the shock compression pressure allowable for the viscosity measurement does not exceed 10 GPa.

Experimental Data

The objects of the experimental study are DMF (C_3H_7ON) "pure" with $\rho_0 = 0.96$ g/cm³, glycerine $C_3H_5(OH)_3$ "Pure for Analysis" with $\rho_0 = 1.26$ g/cm³, and distilled water with $\rho_0 = 1.0$ g/cm³. For $t_0 = 18$°C their viscosities were 0.00786 [15], 18, and 0.01 P, respectively. The shock parameters in water, glycerine, and DMF were found by means of the experimental mass flow rates and D are the Hugoniot u-relations: for water $D = 1.593 + 1.8u$ [19], for glycerine $D = 1.91 + 2.41u - 0.21u^2$, [4], for DMF $D = 1.650 + 2u - 0.06u^2$ on the generalized adiabat from [20].

Explosive charges 100 mm high and 84 mm in diameter, initiated by a plane wave generator were used to reach shock pressures of 6-10 GPa as in [10]. After the plane detonation front emergence on the charge endface, broadening of the explosion products in the 10-mm air gap and their deceleration occurred on a 1.5 mm thick screen boundary of silicate glass covering the fluid. The aluminum foil cylindrical conductors and stream velocity sensors were placed at a 8-12 mm depth from the inner screen boundary. The stream velocity remained constant for

TABLE 1

t_0, °C	η_0, P	u, km/sec	p, GPa	t, °C	η, P
20	15.14	0.173	0.50	41	30(25—35)
19	16.49	0.185	0.55	41	30(20—40)
21	13.91	0.203	0.61	46	25(20—30)
19	16.49	0.207	0.63	44	45(40—50)
20	15.14	0.430	1.60	82	80(30—100)
20	15.14	0.550	2.2	105	50(30—100)
23	11.79	0.590	2.4	115	30(10—50)
20	15.14	1.16	6.5	260	15(10—20)
19	16.49	1.58	10.3	404	20(10—50)

TABLE 2

t_0, °C	η_0, P	u, km/sec	p, GPa	t, °C	η, P
48	1.98	0.340	1.2	95	<1
70	0.58	0.615	2.6	167	<0.5
52	1.55	1.30	7.7	336	15(5—20)
—3	146.46	0.50	1.9	72	>200
0	104.56	1.26	7.3	271	20(10—30)
—11	387.33	0.330	1.1	28	>200
—10	340.83	1.24	7.2	275	20(10—30)
—8	265.40	1.29	7.6	293	15(5—20)

1.5-3 μsec after the sensors intersected the shock front in such a formulation of the experiments.

The characteristic curves of cylinder entrainment in the upper pressure range are presented in Fig. 4 in the dimensionless variables $\bar{v}$, $\bar{\tau}$, where the velocity scale is the fluid mass flow rate u and the time is r/u. Curve 2 is obtained in a test with DMF for t_0 = 20°C, u = 1.53 km/sec, and p = 6.7 GPa. Its computation is shown by the dashed lines (the numbers near them are the viscosity values). An experimental dependence for DMF is found below the allowable domain of definition η bounded by the computed curve with η = 1 P. This result does not contradict the data on the conductivity. According to [3], the viscosity of DMF for a 4 GPa shock pressure grows seven times, i.e., to η = 0.05 P. Curves 1 and 3 characterize the rheology of shock-compressed water for u = 1.50 km/sec, p = 6.47 GPa (t_0 = 20°C, η_0 = 0.01 P) and glycerine for u = 1.16 km/sec, p = 6.3 GPa (t_0 = 18°C, η_0 = 18 P). The close location of the curves indicates almost total agreement of their rheological characteristics in the shock-compressed state. For a dynamic pressure of 6.5 GPa, the viscosities of glycerine and water are within the limits 10-40 P.

All the results of the glycerine investigation are presented in Tables 1 and 2. The data of Table 1, obtained for an initial glycerine temperature of t_0 = 19 ± 2°C and η_0 ~ 14-20 P characterize the shock compression temperature, the stream velocities, the Hugoniot temperature, and the possible limits and the most probable values of the viscosity (last column). Moreover, information about the initial temperatures and viscosities of three series of tests executed with glycerines heated to 50-70°C and cooled to −3 to −11°C is contained in the first two columns of Table 2. The viscosities for 6-10 GPa are almost identical independently of the temperature ahead of the shock front because of the closeness of the thermodynamic parameters of the compressed states for a common temperature rise.

On the other hand, for p ~ 1 GPa the viscosities of the heated and cooled glycerines differ just as strongly as at atmospheric pressure. For t_0 = 50-70°C the value of η lies below, and for t_0 = −11°C above, the measurement limits. For cooled glycerine the values of η at p ~ 1.5 GPa are estimated by the shock front shape as determined by the foil sensor. A careful comparison of the oscillograms of Fig. 1 with the shock front configurations in DMF, water, and heated glycerines established the "instrumental" magnitude of the front droop ~0.3 μsec and the additional spread in glycerine 0.1-0.2 μsec. The physical nature of this spread is due to the structure of the shock front in media with high viscosity.

It is known [16] that the relation between the viscosity and the shock front width has the form

$$\rho_0 D T_0 (S - S_0) \sim \eta u^2 / \delta x. \tag{3}$$

Here δx is the front width, S_0 and S are the initial and final entropies of the substance, and ρ_0 is the initial density.

For a weak shock

$$T_0 (S - S_0) = u^3 D' / D, \tag{4}$$

where D' is the derivative with respect to the mass flow rate, and D is the u-relationship. Substituting (4) into (3) we obtain

$$\eta \sim \rho_0 u D' \delta x. \tag{5}$$

Replacing δx by Dδτ (δτ is the viscous spread of the front in time) results in the simple formula

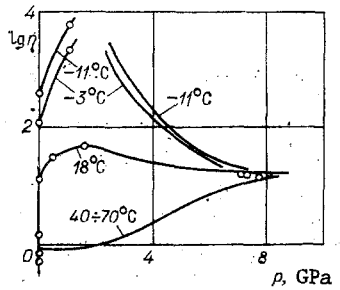

Fig. 5

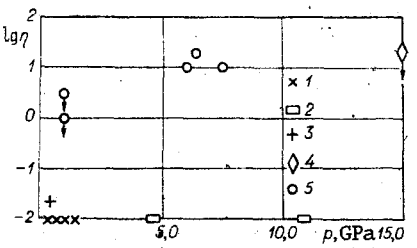

Fig. 6

$$\eta \sim D' p \delta\tau \ (p = \rho_0 D u), \tag{6}$$

For glycerine D' = 2.41-0.42u.

In one of the tests with glycerine for $t_0 = -10°C$ ($T_0 = 263°K$), u = 0.330 km/sec, p = 1.12 GPa, $\delta\tau \sim 1.5 \cdot 10^{-7}$ sec. Hence from (6) we have an estimate of the quantity $\eta \sim 3.8 \cdot 10^3$ P and this viscosity corresponds to the effective front temperature $T_1 = 0.5(T_0 + T)$. Using (2), we find T = 307°K and by extrapolation in the domain 1.12 GPa of the data in [4], the second estimate of the viscosity in the shock front $\eta \sim 5.0 \cdot 10^2$ P, which is close to the first in magnitude.

The viscosities determined by the AC method for water with $t_0 = 18°C$ ($\eta_0 = 0.01$ P) are extended in Table 3 by also including the data from [10]. The shock compression temperatures presented here in the equation of state [21] are in agreement with the experimental measurements [22, 23]. Up to a pressure of ~2 GPa the viscosity of water is less than 1 P. As the shock compression pressure increases, the viscosity of water grows to 10-25 P and is conserved at this level for a further rise to ~8 GPa.

Discussion of the Results

The tendency to a change in the viscosity of glycerine with a different initial temperature under shock compression is shown in Fig. 5, where the points are experiments. For glycerine with $t_0 = 18°C$ the left section of the curve to p = 2 GPa reproduces the viscosity calculated from static data and their nearby extrapolation. The values of $\eta = 53$ P for p = 1.6 GPa as the pressure rises to ~7-10 GPa are lowered to a level ~20 P. The viscosities of both the heated and the cooled glycerines approach this same limit. Such a result is a natural consequence of the rise and drawing together of Hugoniot temperatures for different t_0 as the shock amplitude increases. On the other hand, at lower pressures the viscosities of glycerine with $t_0 = 70$ and $-11°C$ differ by approximately four orders.

The main factor [6] governing the viscosity of a fluid under pressure is the activation enthalpy H needed to the activated flow state. By definition $H = E + p\Delta\vartheta$. In this binomial E is the activation energy specified by the forces of intramolecular interaction, while $p\Delta\vartheta$ is the work against the external pressure force. After division by the Avogadro number, the quantity $\Delta\vartheta/N$ is the increase in the volume of vacancies needed for the migration of adjacent molecules. Ordinarily $\Delta\vartheta/\vartheta = n^{-1}$ is a small fraction of the molecular volume. The results of static measurements of the viscosity in [4] and of ours permit the activation enthalpy and the value of $\Delta\vartheta$ in the extended band of parameters to be found.

On the basis of the known equation [6]

$$\eta = \text{const}\, \sigma^{2/3} T^{3/2} \exp\left(\frac{E + p\Delta\vartheta}{RT}\right), \tag{7}$$

where $\sigma = \vartheta_0/\vartheta$; ϑ_0, ϑ is the fluid volume in the initial and compressed states from which

TABLE 3

u, km/sec	p, GPa	t, °C	η, P	u, km/sec	p, GPa	t, °C	η, P
0.400	0.92	52	<3	1.45	6.09	316	20(5—40)
0.426	1.0	54	<1	1.49	6.37	333	25(5—40)
0.430	1.02	55	<3	1.50	6.44	338	20(5—40)
0.440	1.05	56	<1	1.65	7.52	405	10(5—20)

TABLE 4

p, GPa	Δϑ	n	Δϑ	n	Δϑ	n	η, P	H, kcal	η, P	H, kcal
	t, °C									
	20		80		150		50		112	
0	16.63	4.38	13.42	5.43	9.68	7.54	1.10	13.67	0.1	9.07
0.4	12.67	5.39	9.61	7.11	7.68	8.90	8.2	16.54	0.4	11.47
0.8	10.82	6.07	8.60	7.63	7.51	8.74	40.4	19.11	1.1	13.32
1.2	8.91	7.16	7.88	8.08	6.72	9.48	164.0	20.0	3.0	15.0
1.6	7.95	7.83	5.75	10.84	5.18	12.03	468.7	21.17	6.7	16.22
2.0	6.01	10.20	5.79	10.5	4.55	13.43	1339.4	22.37	14.9	17.5

$$\Delta\vartheta = \left| \frac{d \ln (\eta\sigma^{-2/3})}{d (p/RT)} \right|_T; \tag{8}$$

$$H = \left| \frac{d \ln (\eta T^{-3/2})}{d (RT)^{-1}} \right|_\sigma. \tag{9}$$

The sample values of H and Δϑ obtained by graphical differentiation of the data in [4] are presented in Table 4. Equation (7) in combinations of σ, T, η, and H permits finding the numerical value of the constants and then determining H for other known values of σ, T, and η. The activation enthalpy found in such a manner for glycerine under a 6.5 GPa shock pressure and 530°K temperature turned out to equal 24 kcal/mole. According to the estimate, for n = 7-10 approximately 12 kcal is for the work against the external pressure force and ~10-14 kcal is for the internal activation energy.

For glycerine and other compounds containing two or more hydroxyl groups, the anomalously high viscosity and high activation energy are explained by the existence of hydrogen bonds of hydrogen bonds that should be destroyed for the formation of activated flow states. The energy needed to rupture the hydrogen bonds is called the "structural activation energy." As the temperature increases the number of hydrogen bonds that should be ruptured and the structural component in the quantity E diminish. However, as our results showed, at high pressures and high shock compression density, its role is substantial up to 600°K temperatures and higher. The same sequence in the change in energy and activation enthalpy also determines the ion mobility in electrolytes for glycerine as follows from the data in [4] on the reduction of its impurity conductivity under shock compression.

Another situation is detected in water under analogous conditions. The results of different methods of determining its viscosity under static and shock pressures and compared in the semi-logarithmic $\log\eta - p$ diagram in Fig. 6. The results [8] obtained by the corrugated front method do not fall in the field of the diagram and are apparently strongly exaggerated. According to [5], "it is difficult to show that the viscosities of shock-compressed water, mercury, aluminum, and lead are in agreement. Damping of the perturbations of the curved front should be a result of complex shock interactions that differ from the hypothesized simple viscous dissipation." The viscosity of water is determined by static experiments [14] (points 1) for $\eta = 10 \cdot 10^{-2}$ P on the horizontal axis of Fig. 6, and above 40 GPa by the electrolyte conductivity [1, 2] (points 2). In a test [11] (point 3) the upper values for the front thickness and the viscosity that do not contradict the static data are obtained by means of the intensity of the light reflection from the shock front. Estimates made by means of the coagulation rate in [12] (point 4) for p = 15 GPa are the upper bound. The results of this paper and [10] are denoted by the points 5.

To understand the physical situation, the determination of the viscosity [10] by the AC method for 6-7 GPa is of value in principle. The viscosity of water close to the viscosity of glycerine exceeds by an order or more the viscosity of DMF and differs by three orders at the higher side from the ion mobility estimate. This is related to the difference mechanism of impurity ion migration over the vacancies and the displacement of the consolidated "flow units" of the structurally bound water molecules. As mathematical modeling by the method of molecular dynamics shows, under normal conditions [24] water has an open structure with coordination number (CN) 5.5 for the nearest neighbors. As the density rises to 1.346 g/cm³ and the temperature to 97°C (the Hugoniot state for 2.5 GPa), the CN increases to 11-12 according to [25]. However, at a spacing of the molecule diameter, only four adjacent molecules are located in the separated tetrahedral directions. In the compressed state, water therefore forms a three-dimensional polymer structure with curved mutually penetrating but unruptured hydrogen bonds. An indication of the destruction of the polymer structure and

transformation of water into a simple fluid of free molecules [19] is the breakpoint of the shock adiabat at a 10-12 GPa pressure. Up to these pressures the viscosity of water is anomalously high because of the large number of hydrogen bonds which should be ruptured for the formation of activated flow states.

The authors are grateful to V. V. Yakushev for multiple and fruitful discussions of many aspects of the research.

LITERATURE CITED

1. S. D. Hamann and M. Linton, "The viscosity of water under shock compression," J. Appl. Phy., 40 (1969).
2. S. D. Hamann and M. Linton, "Electrical conductivity of water in shock compression," Trans. Faraday Soc., 62 (1966).
3. S. S. Nabatov, V. M. Shunin, and V. V. Yakushev, "Viscosity of liquid inert and explosive substances behind a shock front," in: Chemical Physics of the Combustion and Explosion Process Detonation [in Russian], Chernogolovka (1977).
4. A. N. Dremin, D. I. Kuznetsov, et al., "Viscosity and electrical conductivity of glycerine under high dynamic and static pressures," Zh. Fiz. Khim., 54, No. 1 (1980).
5. S. D. Hamann and M. Linton, "Electrical conductivities of shock-compressed solutions of KI in organic solvents," J. Chem. Soc. Faraday Trans., 74, (1978).
6. Glasstone, C. Leiter, and H. Eyring, Theory of Absolute Reaction Rates [Russian translation], IL, Moscow (1948).
7. A. D. Sakharov, R. M. Zaidel', et al., "Experimental investigation of shock stability and the mechanical properties of a substance at high pressures and temperatures," Dokl. Akad. Nauk SSSR, 159, No. 5 (1964).
8. V. N. Mineev and R. M. Zaidel', "Viscosity of water and mercury under shock loading," Zh. Eksp. Teor. Fiz., 54, No. 6 (1968).
9. L. V. Al'tshuler, G. I. Kanel', and B. S. Chekin, "New measurements of the viscosity of water behind a shock front," Zh. Eksp. Teor. Fiz., 72, No. 2 (1977).
10. G. Kh. Kim, "Measurement of the viscosity of shock-compressed water," Zh. Prikl. Mekh. Tekh. Fiz., No. 5 (1984).
11. P. Harris and H. N. Presley, "Reflectivity of a 5.8 kbar shock front in water," J. Chem. Phys., 74 (1981).
12. O. B. Yakusheva, V. V. Yakushev, and A. N. Dremin, "Formation of sulfur particles in sodium thiosulfate solutions behind a shock front," Combustion and Explosion [in Russian], Materials of the Third All-Union Symp. on Combustion and Explosion, Nauka, Moscow (1972).
13. L. V. Al'tshuler, "Application of shocks in high pressure physics," Usp. Fiz. Nauk, 85, No. 2 (1965).
14. K. E. Bett and J. B. Cappi, "Effect of pressure on the viscosity of water," Nature, 207 (1965).
15. R. S. Reed, D. M. Prausnitz, and T. C. Sherwood, Properties of Gases and Liquids [Russian translation], Khimiya, Leningrad (1982).
16. Ya. B. Zel'dovich and Yu. P. Raizer, Physics of Shocks and High-Temperature Hydrodynamics Phenomena [in Russian], Nauka, Moscow (1966).
17. N. A. Gumerov, "Unsteady viscous incompressible fluid flow around a cylinder at low Reynolds numbers," Vestn. Mosk. Gos. Univ., Ser. 1, Matematika, Mekhanika, No. 2 (1983).
18. D. J. Tritton, "Experiments on the flow past a circular cylinder at low Reynolds numbers," J. Fluid Mech., 6 (1959).
19. I. I. Sharipdzhanov, L. V. Al'tshuler, and S. E. Brusnikin, "Shock and isentropic water compressibility anomalies," Fiz. Goreniya Vzryva, No. 5 (1983).
20. A. N. Afanasenkov, V. M. Bogomolov, and I. V. Voskoboinikov, "Generalized shock adiabat of organic fluids," Fiz. Goreniya Vzryva, No. 4 (1967).
21. M. Cowperthwaite and R. Shaw, "Equation of state for liquids calculation of the shock temperature of carbon tetrachloride, nitromethane, and water in the 100 kbar region" J. Chem. Phys., 53 (1976).
22. S. B. Kormer, "Optical investigations of properties of shock-compressed dielectrics," Usp. Fiz. Nauk, 94, No. 4 (1963).
23. G. A. Lyzenga and T. J. Ahrens, "The temperature of shock-compressed water," J. Chem. Phys., 76 (1982).
24. R. W. Impey, M. L. Klein, and I. R. McDonald, "Molecular dynamics studies of the structure of water at high temperatures and density," J. Chem. Phys., 74 (1981).

25. F. H. Stilinger and A. Rahman, "Molecular dynamics study of liquid water under high compression," J. Chem. Phys., 61 (1974).

CRACK GENERATION AND PROPAGATION MECHANISM

V. V. Struzhanov

UDC 539.3

As the load increases, a solid body goes over from one stable equilibrium position to another. The dynamic opening of cracks can be treated as buckling with a subsequent jump-like passage to a new stable position. Consequently, the mathematical methods of studying the equilibrium, stability, and buckling of mechanical systems, in particular the apparatus of catastrophe theory, can be used to analyze the carrying capacity, crack formation and propagation, and rupture. As has been noted in [1], the descending branches of the laws of system element interaction are here of substantial value since they permit the determination of all the possible equilibrium positions.

In this paper, an approach based on studying equilibrium positions by catastrophe theory methods is used to analyze the behavior of some of the simplest discrete models of a solid in the form of atomic lattices subjected to load. The process of crack formation and opening is represented graphically up to rupture.

1. Let us first examine a model representing several parallel series of atoms (Fig. 1a). The interaction force between the first two series, referred to the unit of length of these series is given by the function [1]

$$\Phi = Ex \exp(-x/x_f),$$

where x is the magnitude of the change in the distance between series, x_f is the value of x corresponding to the maximal force, and E is Young's modulus. In contrast to [1], we assume that in removing the load the interaction force changes according to the linear law $E(x - x_e)$ for fixed x_e. Here x_H is the inelastic component of the displacement x, $x_H = x[1 - \exp \times (-x/x_f)]$. The interaction force between the series b and d referred to the length unit is determined by the expression $\Phi' = Ec^{-1}y$, where y is the magnitude of the change in spacing, and c is a numerical parameter taking account of the pliability of the system of atomic series between b and d. The higher such series, the higher the value of c.

Keeping the series a fixed, we stretch the system quasistatically by giving a displacement u to the series d (stiff loading). The strain potential energy here is

$$\Pi = \int_0^x \Phi dx + (u - x)^2 E/2c.$$

It is natural to call the variable x the state parameter and u, c the control parameters. Then the function Π can be considered as a two-parameter family of functions $\Pi: S \times C$, where $S = R$ is the space of states $(x \in S)$, $C = R \times R = R^2$ is the control space $((u, c) \in C)$, and R is the set of real numbers.

The critical points of the function Π are determined by the equation

$$\partial\Pi/\partial x = Ex \exp(-x/x_f) - (u - x)E/c = 0. \quad (1.1)$$

For these values of (u, c) all the equilibrium positions of the system evidently are obtained by solving (1.1). The set of these solutions, the points (x, u, c) form a manifold of the catastrophe M in three-dimensional space [2]. It has the form of a surface with a build-up and is shown in Fig. 1b. Here and henceforth $x_f = 0.4$.

The doubly and triply degenerate critical points are determined form the joint solution of (1.1) and [3]

$$\partial^2\Pi/\partial x^2 = E(1 - x/x_f) \exp(-x/x_f) + E/c = 0 \quad (1.2)$$

Sverdlovsk. Translated from Zhurnal Prikladnoi Mekhaniki i Tekhnicheskoi Fiziki, No. 6, pp. 118-123, November-December, 1986. Original article submitted October 9, 1985.

 0021-8944/86/2706-0894$12.50